Solar Phys
DOI 10.1007/s11207-011-9774-x

Galactic Cosmic Ray Intensity Response to Interplanetary Coronal Mass Ejections/Magnetic Clouds in 1995 – 2009

I.G. Richardson · H.V. Cane

Received: 4 February 2011 / Accepted: 8 April 2011
© Springer Science+Business Media B.V. 2011

Abstract We summarize the response of the galactic cosmic ray (CGR) intensity to the passage of the more than 300 interplanetary coronal mass ejections (ICMEs) and their associated shocks that passed the Earth during 1995 – 2009, a period that encompasses the whole of Solar Cycle 23. In $\sim$80% of cases, the GCR intensity decreased during the passage of these structures, *i.e.*, a "Forbush decrease" occurred, while in $\sim$10% there was no significant change. In the remaining cases, the GCR intensity increased. Where there was an intensity decrease, minimum intensity was observed inside the ICME in $\sim$90% of these events. The observations confirm the role of both post-shock regions and ICMEs in the generation of these decreases, consistent with many previous studies, but contrary to the conclusion of Reames, Kahler, and Tylka (*Astrophys. J. Lett.* **700**, L199, 2009) who, from examining a subset of ICMEs with flux-rope-like magnetic fields (magnetic clouds) argued that these are "open structures" that allow free access of particles including GCRs to their interior. In fact, we find that magnetic clouds are more likely to participate in the deepest GCR decreases than ICMEs that are not magnetic clouds.

Keywords Interplanetary coronal mass ejections · Magnetic clouds · Cosmic rays · Solar wind plasma · Interplanetary magnetic field · Coronal mass ejections

1. Introduction

Short term ($<\sim$ 1 week duration) decreases, typically of a few percent, in the intensity of galactic cosmic rays (GCRs) were first observed by Forbush (1937) and Hess and Dem-

I.G. Richardson (✉) · H.V. Cane
Code 661, NASA/Goddard Space Flight Center, Greenbelt, MD 20771, USA
e-mail: ian.g.richardson@nasa.gov

I.G. Richardson
CRESST and Department of Astronomy, University of Maryland, College Park, MD 20742, USA

H.V. Cane
School of Mathematics and Physics, University of Tasmania, Hobart, Tasmania, Australia
e-mail: hilary.cane@utas.edu.au

Published online: 12 May 2011

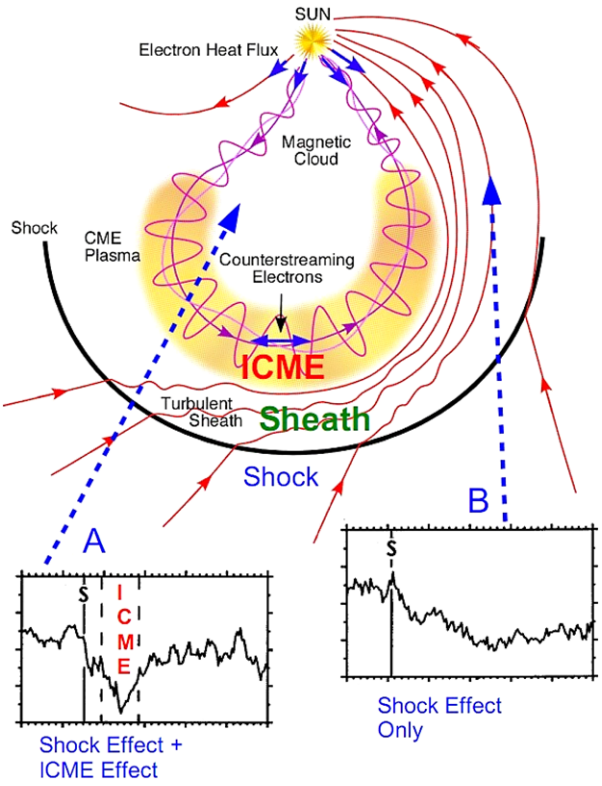

Figure 1 Schematic of an interplanetary coronal mass ejection driving a shock ahead of it and the associated variations in the galactic cosmic ray intensity along trajectories that do (A) or do not (B) encounter the ICME (adapted from Cane, 2000 and Zurbuchen and Richardson, 2006).

melmair (1937) using ionization chambers. They were later shown, using neutron monitors (NMs), to originate in the interplanetary medium (Simpson, 1954) and to be of two types: "Recurrent", which recur with the solar rotation period and are associated with corotating high-speed streams (for a review see Richardson, 2004 and references therein), and "non-recurrent", caused by the passage of transient solar wind structures associated with coronal mass ejections at the Sun. The focus of this paper is the latter class of events, often termed "Forbush decreases" (FDs), though this term is also used by some researchers to refer to recurrent decreases.

The properties and interplanetary drivers of FDs have been reviewed by Cane (2000). Figure 1 shows a schematic of a fast interplanetary coronal mass ejection (ICME), the manifestation in the solar wind of a coronal mass ejection at the Sun such as may be observed by coronagraphs, driving a shock ahead of it. Two processes may contribute to the decrease in GCR intensity (see, *e.g.*, Barnden, 1973a, 1973b; Wibberenz *et al.*, 1998). The first is a decrease of the GCR radial diffusion coefficient in the turbulent "sheath" between the shock front and leading edge of the ICME. The resulting intensity-time profile is a linear decline during sheath passage followed by a recovery (*cf.*, Figure 2 of Wibberenz *et al.*, 1998).

The second process arises from the at least partially closed magnetic configuration of ICMEs as evidenced for example by the presence of bi-directional suprathermal electron flows in many ICMEs suggesting that magnetic field lines are rooted at the Sun at both ends (see, *e.g.*, Gosling *et al.*, 1987; Shodhan *et al.*, 2000). GCRs enter the interior of the ICME as it moves away from the Sun by, for example, cross-field diffusion and gradient and curvature drifts (see, *e.g.*, Krittinatham and Ruffolo, 2009; Kubo and Shimazu, 2010) such

that the "ICME effect" is indicated by a local decrease in the GCR intensity as the ICME moves over the observer.

The ICME in Figure 1 includes helical magnetic field lines with a flux-rope-like configuration characteristic of the subset of ICMEs known as "magnetic clouds" (Klein and Burlaga, 1982) that have enhanced magnetic fields that rotate slowly in direction as the structure moves past the observer. A simple model discussed by Cane, Richardson, and Wibberenz (1995) and Vanhoefer (1996) suggests that for a magnetic cloud with a flux rope of radius a and speed V away from the Sun, the maximum GCR depression inside the magnetic cloud is a monotonically-decreasing function F of the cloud parameters, $\Delta U/U_{\rm o} = F(K_{\perp} r/Va^2)$, where r is the distance from the Sun, and $K_{\perp}$ is the perpendicular diffusion coefficient. If $K_{\perp}$ is assumed to be proportional to $1/B$, where B is the strength of the magnetic field in the ICME, the size of the depression decreases monotonically with the product BVa^2. Thus, the depression size is expected to be smaller for a magnetic cloud that is slower (there is more time for particles to fill the MC), smaller, includes weaker magnetic fields, and is further from the Sun. Vanhoefer (1996) expressed the filling rate in terms of a characteristic time $t_{\rm c} \propto a^2/K_{\perp}$, and inferred $K_{\perp} \sim 10^{18}$ to 10^{19} cm^2 s^{-1} for ~ 1 GeV protons. This is around 2 – 3 orders of magnitude smaller than the Palmer (1982) "consensus value" of $\sim 10^{21}$ cm^2 s^{-1} in the undisturbed solar wind which in turn is reasonably consistent with values obtained from recent modeling (Shalchi *et al.*, 2010). *Ulysses* spacecraft observations made at 3.4 – 4.6 AU from the Sun (Bothmer *et al.*, 1997) demonstrate that GCR decreases associated with ICMEs persist well beyond Earth's orbit, and may be larger than expected from this simple model perhaps due to substantial expansion of the ICME (Wibberenz *et al.*, 1998).

Figure 1 shows two possible trajectories relative to the shock/ICME. Along trajectory A, the shock is encountered first followed later by the ICME, then a return to the region of post-shock field lines connected to the shock. Along this trajectory, both the shock and ICME effects would be expected to be present, producing an initial decrease in GCR intensity following the shock, then a local decrease during passage of the ICME, followed by a recovery on return to the post-shock plasma. Such features are evident in the representative GCR intensity-time profile observed by a neutron monitor (NM) shown in Figure 1. Depending on the change in diffusion coefficient at the shock, the ICME properties, and the observer's trajectory relative to these structures, the relative sizes of the "first step", associated with the shock effect, and the "second step", associated with the ICME may vary from case to case. For a slow ICME that generates only a weak or no shock, the first step may be weak or absent. Along trajectory B in Figure 1, the ICME is not encountered. Only the shock effect is present, producing a GCR intensity decrease commencing at the shock followed by a slow recovery that may extend over several days, as illustrated in the sample neutron monitor data for such a situation.

In the past, the relative importance of the shock and ejecta effects was a matter of some debate. For example, Zhang and Burlaga (1988) and Lockwood, Webber, and Debrunner (1991) concluded that magnetic clouds have little effect on the cosmic ray intensity. On the other hand, other studies (see, *e.g.*, Badruddin, Yadav, and Yadav, 1986; Sanderson *et al.*, 1990) concluded that magnetic clouds can make an important contribution to FDs. Major reasons for this confusion included event-to-event variability, and the use of observations from a single neutron monitor to relate GCR variations and interplanetary structures. Such observations will be complicated by the presence of diurnal intensity variations because of the rotation of the Earth.

In Cane (1993) and subsequent studies (see, *e.g.*, Cane *et al.*, 1994; Cane, Richardson, and Wibberenz, 1997; Richardson, 1997), we used the counting rates of the large volume plastic scintillator anti-coincidence guards of the Goddard Medium Energy (GME) instrument on the IMP 8 spacecraft and the University of Kiel experiments on the *Helios 1* and *2*

spacecraft (located in heliocentric orbits ranging from 0.3 to 1 AU from the Sun) to study GCR variations at multiple locations in the inner heliosphere during the passage of individual shocks and ICMEs. These studies verified the scenario presented in Figure 1 in which both the shock and ICME effects contribute, depending on the spacecraft trajectory relative to these structures. We also demonstrated that, as expected, the particle intensity inside ICMEs increases with heliocentric distance.

In the present study, we examine the GCR response to the more than 300 ICMEs that passed Earth during Solar Cycle 23 identified in our "comprehensive" catalog of such events (Cane and Richardson, 2003; Richardson and Cane, 2010a), and hence summarize the behavior of the GCR intensity during the passage of a large sample of ICMEs and their related shocks. This study is motivated in part by a recent paper (Reames, Kahler, and Tylka, 2009) that questions the role of magnetic clouds in FDs and concludes that magnetic clouds "contain no structures that are magnetically closed to the penetration of ions with energies above a few MeV amu^{-1}" including GCRs. We will briefly respond to this claim in Section 4.

In the next section we will discuss the instrumentation used in this study. Section 3 will outline the properties of FDs associated with ICMEs and magnetic clouds in 1995 – 2009. Section 4 summarizes and discusses these results.

2. Instrumentation and Example Event

In this study, we use GCR observations from two sources. The first is the anti-coincidence guard of the Goddard Medium Energy (GME) instrument on the IMP 8 spacecraft (McGuire, von Rosenvinge, and McDonald, 1986). IMP 8 was launched in October, 1973 into a $\sim 40 R_e$ geocentric orbit. The spacecraft operated until October, 2006 but data coverage was considerably reduced after the official end of the mission in October 2001; data after this time were acquired as part of the *Voyager* spacecraft project. This study uses data up to the end of 2005. The GME guard (detector G) was not intended to be used for scientific studies, so the energy response and geometrical factor are not well determined. Nevertheless, our previous studies have clearly demonstrated that the guard counting rate provides a useful measure of the GCR intensity-time variations at the spacecraft at least at times when the rate is not dominated by solar particle events. Comparison with intensity-time profiles at various energies during solar particle events suggests that the lower energy threshold of the guard is ~ 60 MeV. As discussed by Richardson, Cane, and Wibberenz (1999), the guard rate is highly correlated with the GCR intensity measured by the GME 121 – 230 MeV proton channel which has been carefully corrected for instrumental effects so as to provide a long-term 1 AU baseline for the *Voyager* mission (see Figure 10 of Richardson, Cane, and Wibberenz, 1999). The amplitude of the long-term (solar cycle) cosmic ray modulation observed by the guard ($\sim 70\%$; *cf.* Figure 5 of Richardson, 2004) suggests that the guard response is intermediate between that of the 121 – 230 MeV proton channel (modulation amplitude $\sim 90\%$) and mid-latitude neutron monitors ($\sim 20\%$).

Although the guard attributes are not well defined, the guard counting rate has important advantages over neutron monitor observations when comparing intensity variations during FDs with local solar wind structures, specifically the lack of diurnal variation and lower energy response since FDs are known to be larger at smaller energies/rigidities (see, *e.g.*, Cane, Richardson, and Wibberenz, 1995 and references therein). The guard count rate (several hundred counts/s) is several orders of magnitude higher that that of the 121 – 230 MeV proton channel of GME, providing the statistical accuracy necessary to identify GCR modulations of the order of a few % typical of FDs using data accumulation periods that are short

compared to the duration of the FD and associated interplanetary structures. In this study, we use 30-minute averages of the guard rate, providing a statistical accuracy of $\sim 0.1\%$.

Since guard data are not available for many of the ICMEs to be studied, and in some cases, the guard rate is dominated by solar particle events so that the behavior of GCRs cannot be determined, we also use GCR data from the Bartol Research Institute neutron monitor at Thule (located at 76.5°N, 68.7°W). The neutron monitor location near the geomagnetic north pole results in a low energy threshold and reduced diurnal variation well suited for comparison with the guard data. We use 1-hour averaged pressure-corrected data from the Bartol Research Institute website (http://neutronm.bartol.udel.edu/).

To place the GCR observations in context, we use 1-minute averaged near-Earth solar wind magnetic field and plasma data from the OMNI data base (http://spdf.gsfc.nasa.gov/) and 64s-averaged field and plasma data from the *Advanced Composition Explorer* (ACE) spacecraft, available from the ACE Science Center (http://www.srl.caltech.edu/ACE/ASC/). ACE is in orbit around the L1 point ~ 1.5 million km upstream of the Earth. The solar wind transit time from ACE to the vicinity of the Earth is typically $<\sim 1$ hour. We also use solar wind composition and charge state observations from the SWICS instrument on ACE. The typical signatures of ICMEs and magnetic clouds in these data were discussed in Richardson and Cane (2004) although some of the results of that study require revision because of a subsequent reanalysis of the SWICS data that identified additional ion charge states and redefined some element abundance ratios (Richardson and Cane, 2010b). We have previously used these and other data (*in situ* signatures of ICMEs are summarized by Zurbuchen and Richardson, 2006) to compile a catalog of the ~ 340 near-Earth ICMEs during 1996 – 2009 (Richardson and Cane, 2010a). In this study we will focus on the period from 1995, during the solar minimum preceding Solar Cycle 23 to the end of 2009 corresponding to the early rise phase of Cycle 24. For 1995, before the start of our catalog, we consider the magnetic clouds of Shodhan *et al.* (2000).

Figure 2 illustrates how we combine energetic particle and solar wind observations in the vicinity of a shock and magnetic cloud in order to assess how the cosmic ray intensity responds to the passage of these structures. The shock (green vertical line) passed ACE at 09:15 UT and the Earth at 09:48 UT (based on the storm sudden commencement time) on 6 November 2000 (the solar wind observations in Figure 2 are from ACE). It was followed by a sheath of shocked plasma that extended for ~ 12 hours before the arrival of a magnetic cloud, which passed by between 22 UT on this day and 17 UT on 7 November (from the WIND magnetic cloud list compiled by R.P. Lepping (http://lepmfi.gsfc.nasa.gov/mfi/mag_cloud_S1.html)). Evidence of the magnetic cloud includes: the enhanced magnetic field intensity > 10 nT, a smooth rotation in magnetic field direction, here indicated by the polar field direction changing from south of the ecliptic ($\theta < 0°$) to near northward ($\theta \sim 90°$); and abnormally low solar wind proton temperatures ($T_p < 0.5T_{exp}$, indicated by black shading, where T_{exp} (red trace) is the temperature expected from the correlation between solar wind speed and T_p in normal (ambient) solar wind; see Richardson and Cane, 1995 for further discussion of T_{exp}). In addition, there are increases in the solar wind ion charge states (as indicated here by the O^7/O^6 ratio and mean iron charge state) within the ICME.

We also show values of the solar wind suprathermal (272 eV) electron distribution function (multiplied by 10^{29}) with pitch angles $\sim$ parallel (black), anti-parallel (green), and perpendicular (red) to the magnetic field direction (see Section 3 for further details), from the SWEPAM instrument on ACE (http://www.srl.caltech.edu/ACE/ASC/DATA/level3/swepam/). The depression in the intensity of perpendicular electrons and near-balanced parallel and anti-parallel beams in the ICME are indicative of bi-directional suprathermal electron flows. In contrast, the normal anti-solar heat flux is observed in the sheath following the shock.

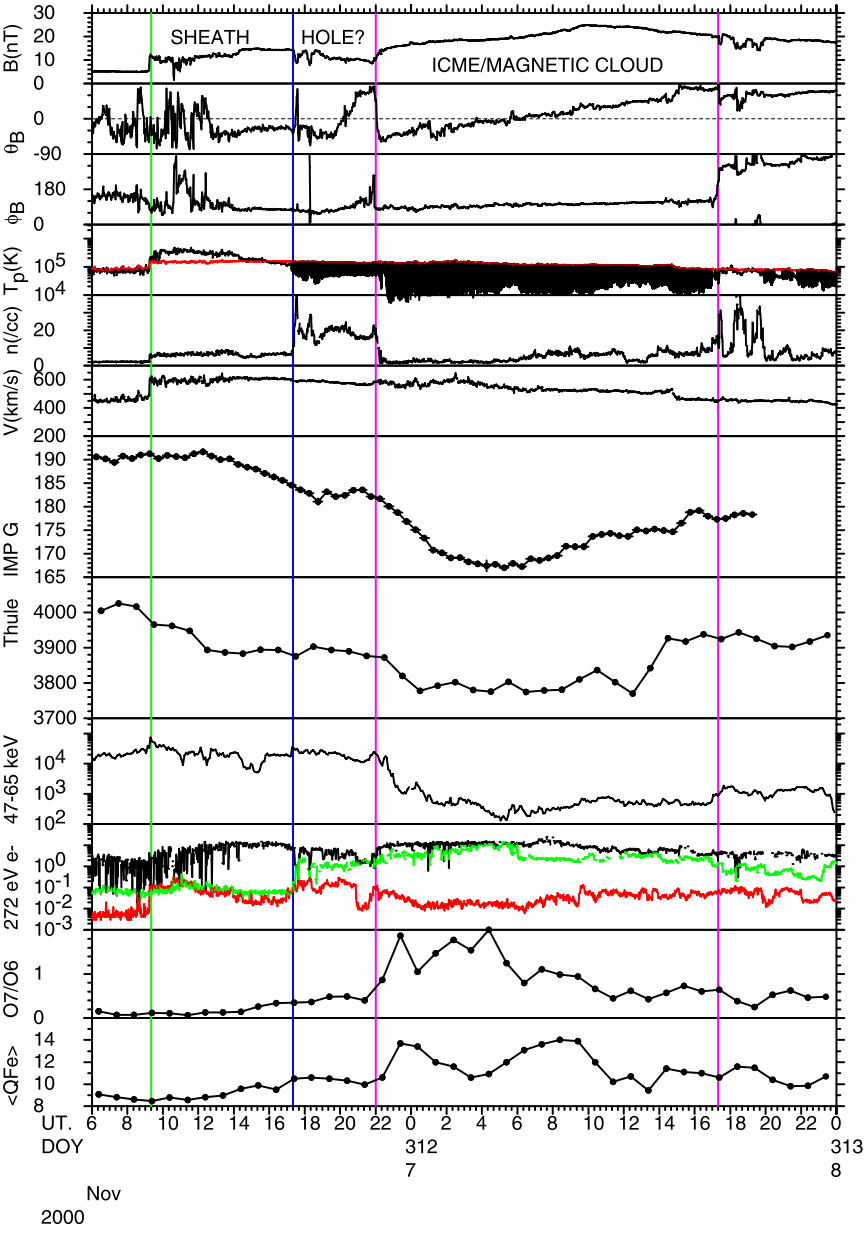

Figure 2 Observations during passage of an ICME and associated upstream shock on 6 – 7 November 2000. The panels show from the top: the IMF intensity and polar and azimuthal angles (in GSE coordinates), solar wind proton temperature, density and speed, GCR observations from the IMP 8 GME guard (G; counts s^{-1}) and the Thule neutron monitor (counts/hr÷100), 47 – 65 keV ion intensity, the solar wind suprathermal (272 eV) electron distribution function ∼parallel (black), anti-parallel (green) and perpendicular (red) to the IMF direction (multiplied by 10^{29}), the solar wind O^7/O^6 ratio and mean Fe charge state. The IMF and solar wind observations are from instruments on the ACE spacecraft. Purple vertical lines indicate the estimated ICME boundaries. The green vertical line is passage of the upstream shock (at ACE). The blue vertical line indicates the start of a magnetic hole-like region ahead of the ICME.

An interesting feature of this particular event is the region immediately ahead of the magnetic cloud with a reduced magnetic field strength possibly with field draping, dense plasma, slightly raised ion charge states, and weak bi-directional suprathermal electron flows. This feature may be related to the magnetic "holes" reported at the leading edges of some magnetic clouds that may be produced by magnetic field line reconnection within ICME structures (*e.g.* Farrugia *et al.*, 2001).

Considering the particle observations, the IMP 8 GME guard rate shows a depression in the sheath that is ∼linear with time (*i.e.*, the "shock effect"), little further change across the "magnetic hole", then a second decrease that commences on entry into the magnetic cloud, reaches maximum depression in the middle of the cloud, and then recovers (*i.e.*, the "ICME effect"). The Thule NM data show a similar pattern with possibly a change in the recovery rate just inside the magnetic cloud trailing edge. The total decrease in the CGR rate, from shock passage to the minimum inside the magnetic cloud, is 12.6% for the guard, and 6% for Thule, reflecting the lower rigidity threshold for the guard. For comparison, the intensity of shock-accelerated 47 – 65 keV ions observed by the EPAM instrument on ACE fell by 99% between the sheath and the center of the cloud, commencing at the passage of the cloud leading edge. Note that both low energy ion and GCR intensities in the "magnetic hole" are similar to those in the sheath, suggesting that this region is most likely magnetically connected to the sheath rather than to the ICME.

3. Results

For each ICME, we measured:

- The total % change in the CGR intensity from shock passage to the minimum intensity measured in the vicinity of the shock/ICME by the IMP 8 GME guard and the Thule neutron monitor. By comparing with the sheath and ICME intervals identified in Richardson and Cane (2010a), we recorded whether minimum intensity occurred in the sheath or ICME.
- The % difference between the GCR intensity at the shock and the minimum in the sheath (the "shock effect").
- The % change from the sheath/ICME boundary to the minimum intensity in the ICME (the "ICME effect").
- *In situ* parameters of the ICME.

Figure 3 summarizes the total GCR variations in the vicinity of the ICMEs as a function of time in 1995 – 2009. The top panel shows the monthly sunspot number. Below are the Thule NM observations for 313 ICMEs, and IMP 8 guard observations for 154 ICMEs. Note that the largest GCR decreases are absent at solar minimum although overall, the FD amplitude does not strictly follow the sunspot cycle. In particular, the largest decrease in this sample observed by Thule occurred on 29 October 2003 during the late decay phase of Solar Cycle 23.

Figure 4 shows distributions of the total GCR intensity change for the Thule NM and IMP 8 guard. The average change was a decrease of 2.2% at Thule, with a maximum decrease of 23%. A decrease in the GCR intensity was observed at Thule in association with ∼80% of the ICMEs and associated shocks, while 12% showed no measurable change (*i.e.* that exceeded the point-to-point variations in the intensity), and 8% exhibited an increase. For the IMP 8 guard, the mean variation was a decrease of 4.3% while the maximum decrease was 30% (note that the large October 2003 FD cannot be measured using the guard

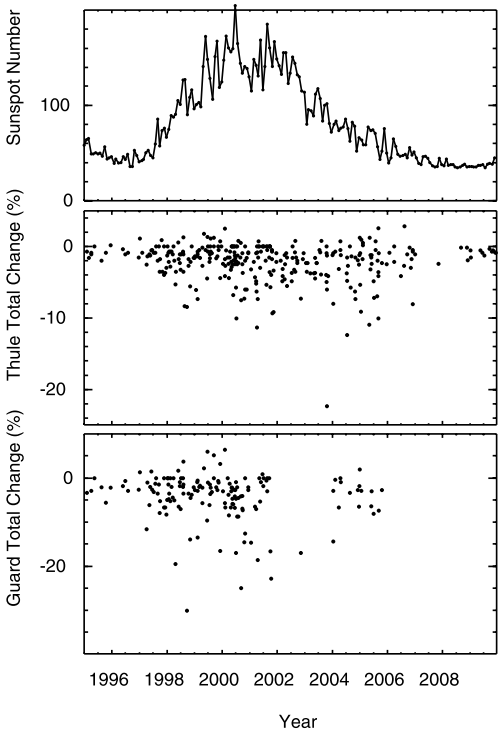

Figure 3 The top panel shows the monthly-averaged sunspot number during 1995 – 2009 encompassing Solar Cycle 23. The bottom panels show the total sizes of individual FDs observed by the IMP 8 guard and Thule neutron Monitor (NM). Note that there are gaps in the IMP 8 data coverage, in particular after late 2001.

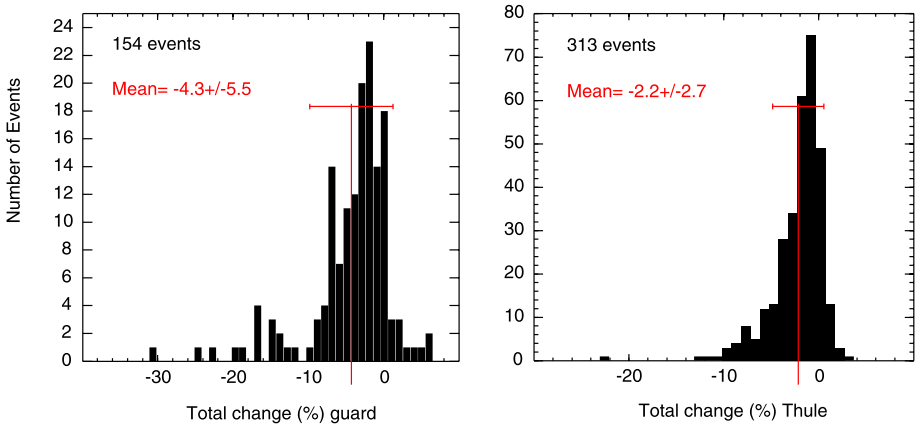

Figure 4 Distribution of total CGR variations in the vicinity of ICMEs in 1995 – 2009 observed with the IMP 8 GME guard and Thule neutron monitor. The mean value and standard deviation are indicated in red.

because of an ongoing solar particle event). Similar percentages of ICMEs were associated with a guard rate decrease (82%), no change (11%) and an increase (7%).

Figure 5 shows that the total change (%) observed by the IMP 8 guard is correlated with the total change measured by the Thule NM ($cc = -0.849$ for 153 events), but around three times larger ($\Delta U_{\mathrm{Thule}} = 0.312 \Delta U_{\mathrm{I8G}} - 0.33$), consistent with the guard measuring

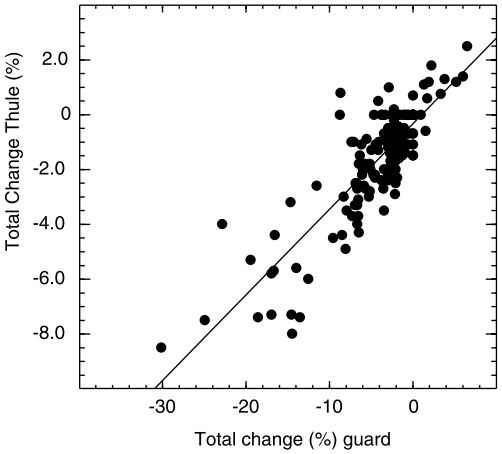

Figure 5 Total GCR intensity change measured by the Thule neutron monitor plotted against the change observed by the IMP 8 guard.

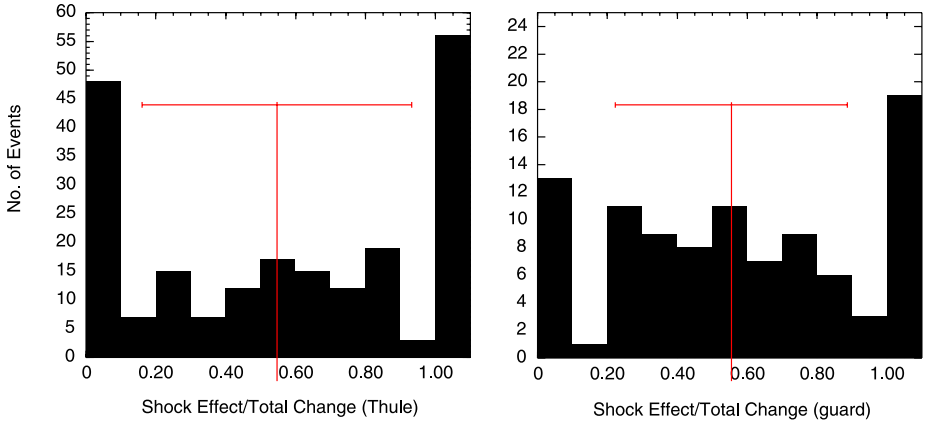

Figure 6 Ratio of the size of the shock effect compared to the total GCR depression size for events observed by the IMP 8 guard or Thule NM. A ratio ~ 1 indicates that the shock effect is dominant, while a ratio ~ 0 indicates that the shock effect is weak/absent. The mean value of the ratio for the guard is 0.56, compared to 0.55 for the Thule NM.

GCR variations but with a lower rigidity threshold than the neutron monitor, as discussed in Section 2. The shock and ICME effects, not illustrated here, show similar relationships between the Thule and guard intensity variations.

We next consider where the minimum CGR intensity was located. Out of 130 events for which the guard data show a decrease and the location of the minimum in the sheath or ICME can be determined, minimum intensity occurred in the ICME in 117 (90%) of these events and in the sheath in 13 events (10%). Similar results are found for Thule: In 207 cases out of 257 events, (81%), minimum intensity was observed in the ICME, while in 50 cases (19%) this occurred in the sheath. Thus, during the passage of ICMEs and their associated shocks, the GCR intensity did not recover following the sheath but reached a minimum in the ICME in a large majority ($\sim 80-90\%$) of these cases. These results clearly indicate that the ICME plays a role in Forbush decreases.

Figure 6 explores this further by comparing the contribution of the shock effect to the total GCR depression. The histograms show the distribution of values for the ratio of the size

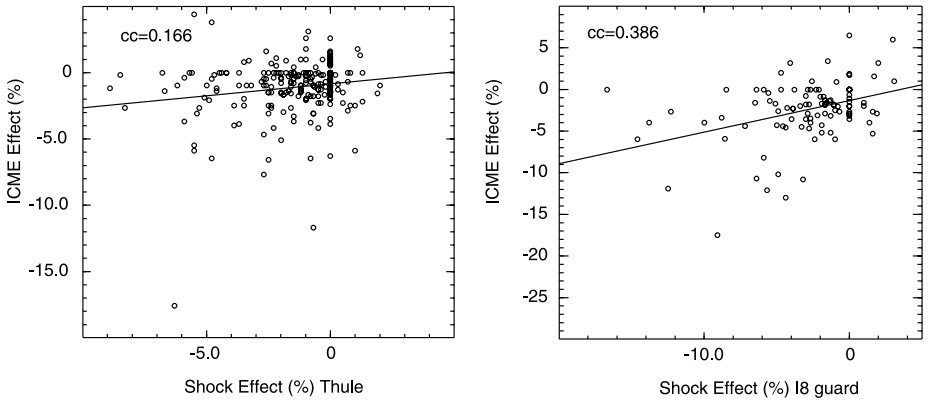

Figure 7 The ICME effect plotted against shock effect for Thule and the IMP 8 GME guard.

of the shock effect to the total decrease for the guard and Thule. A ratio ~ 1 indicates that the shock effect makes the dominant contribution to the total decrease, while ~ 0 indicates that the shock effect is absent and the ICME effect provides the major contribution to the GCR decrease, which then commences with the arrival of the ICME. It is evident that there are large event-to-event variations in the contributions of the shock and ICME effects to the total GCR depression. For Thule, on average, the size of the shock effect is $\sim 55\%$ of the total change (*i.e.*, shock and ICME effects contribute approximately equally on average), while the shock effect is dominant in around a quarter of events, and makes little contribution in a further quarter of events. The IMP 8 guard results are similar though with 20% of events being dominated by the shock effect, and 13% without a shock effect. These results are evidently consistent with the scenario discussed in the introduction in which both shock and ICME effects contribute to Forbush decreases.

Figure 7 shows the size of the ICME effect plotted against the size of the shock effect for Thule and the IMP 8 GME guard. The low correlation coefficients (0.166 and 0.386, respectively) appear to be inconsistent with a scenario in which faster ICMEs are likely to be associated with a larger ICME effect and a stronger shock and more turbulent sheath region, in which case the sizes of the shock and ICME effects might have been expected to show some correlation.

We next examine whether the sizes of the total variation, and shock and ICME effects depend on the properties of the shock and ICME. In our ICME catalog (Richardson and Cane, 2010a), we divide the ICMEs into three types based on their magnetic field signatures. The first group comprises magnetic clouds, which are characterized by enhanced (> 10 nT) magnetic field intensities and slow field rotation through a large angle (Klein and Burlaga, 1982). In general, these events are identified on the WIND magnetic cloud list or by Huttunen *et al.* (2005) but in a few cases the identifications are our own. The second group of ICMEs shows some evidence of a field rotation but the field intensity does not meet the criterion for a magnetic cloud. The third group shows irregular magnetic fields, with no overall organization within the ICME. Figure 8 summarizes how the contributions of each ICME type vary for different ranges of total GCR decrease measured by Thule. For decreases of 1 to 5%, each type of ICME contributes around a third of the events. For decreases of 5 to 10%, around a half involve a magnetic cloud. For the 6 decreases which exceed 10%, 5 of these (83%) involve a magnetic cloud. The results demonstrate the increasingly prominent involvement

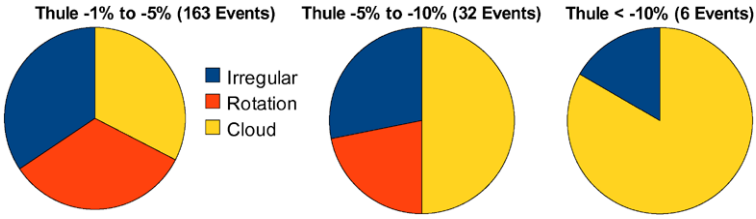

Figure 8 Distribution of ICME type based on magnetic field signatures (Magnetic cloud, evidence of field rotation but lacking other magnetic cloud characteristics, irregular field/no evidence of cloud-like features) associated with Thule FDs in different size ranges. Note the increasing prevalence of magnetic clouds for larger FDs.

of magnetic clouds in FDs of increasing size. A similar trend is found for IMP 8 guard observations.

We have searched for parameters of the ICME and shock that may be correlated with the properties of the Forbush decrease. However, since these can only be measured along a spacecraft's trajectory through these structures, the observed parameters may not be representative of the global properties of the ICME that may be more influential in determining the GCR response. The best correlations we find are between the total FD size and the ICME speed and related parameters. For example, Figure 9 shows the total FD size (Thule) plotted against the *in situ* mean ICME speed, the maximum speed measured in the sheath or ICME, the 1 AU transit speeds of the ICME leading edge and the "disturbance" (the shock, if present, otherwise the ICME leading edge), and the plane of the sky speed of the associated CME observed by the LASCO coronagraphs on the SOHO spacecraft. A correlation with the soft X-ray intensity of the associated flare is also shown. The correlation coefficients are ~ -0.7. Such trends (also evident in the guard data, not shown) are consistent with the expectation that faster CMEs/ICMEs have less time to fill up with GCRs when traveling out to 1 AU.

ICME size and magnetic field strength may also influence FD size, as noted in Section 1. To examine this, we first consider the subset of magnetic clouds. Assuming a simple flux rope configuration, estimates of the cloud diameter and axial magnetic field strength are provided on the WIND spacecraft magnetic cloud list (http://lepmfi.gsfc.nasa.gov/mfi/mag_cloud_S1.html). The left-hand panels in Figure 10 show the sizes of the total decrease, ICME and shock effects at Thule (since there is a larger sample size than for the IMP 8 guard) plotted versus flux rope diameter. The total decrease shows a weak correlation ($cc = -0.443$) with cloud diameter, as does the shock effect ($cc = -0.474$), while the ICME effect, which might be expected to be most strongly influenced by the cloud configuration in fact shows little dependence on the cloud diameter ($cc = -0.138$). Comparing with the axial magnetic field strength (center panels of Figure 10), the total decrease has a weak correlation with axial field ($cc = -0.482$) which arises because the small number of magnetic clouds with large axial fields (> 40 nT) are associated with relatively large depressions. However, the more frequent magnetic clouds with weaker fields are associated with a wide range of decrease size with no clear dependence on the axial magnetic field. A similar situation occurs for the ICME effect and shock effect (which, however, would not be expected to be influenced by the field strength in the following magnetic cloud).

As discussed in the introduction, the GCR depression size associated with passage of a magnetic cloud may scale as BVa^2 (Cane, Richardson, and Wibberenz, 1995). To examine this, we have used the axial field, cloud diameter, and the mean *in situ* speed. The total GCR change at Thule is anti-correlated with the log of BVa^2 ($cc = -0.597$, the highest

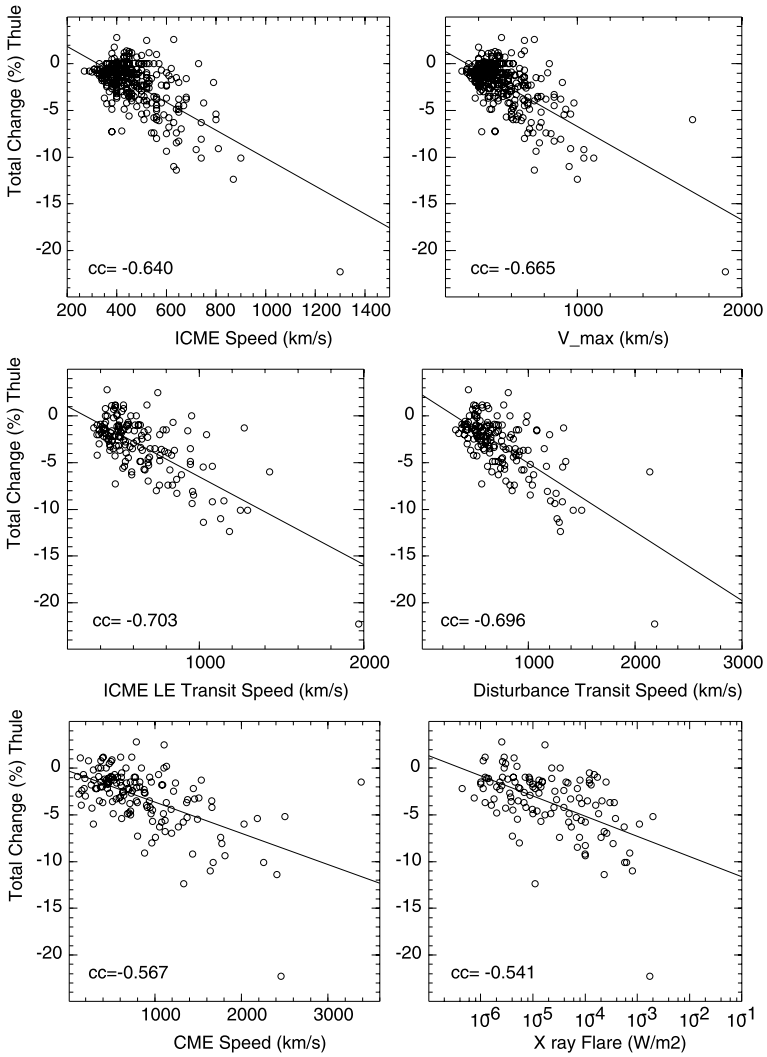

Figure 9 Total FD size (Thule) plotted against the ICME *in situ* speed, maximum speed in the sheath or ICME, ICME leading edge 1 AU transit speed, disturbance (shock, or ICME leading edge if there is no shock) 1 AU transit speed, CME speed observed by LASCO, and the peak soft X-ray intensity of the associated solar flare.

value in Figure 10), with progressively weaker anti-correlations for the shock and ICME effects. Since the dependence on BVa^2 is derived from a model of GCR propagation into a magnetic cloud, we would expect it to be related most closely to the size of the ICME effect. However, this does not appear to be the case for this set of events. Another influence on the decrease size might be the spacecraft trajectory relative to the magnetic cloud. The WIND magnetic cloud list includes the distance of closest approach as a fraction of the cloud radius. However, we find that this parameter does not organize the FD size.

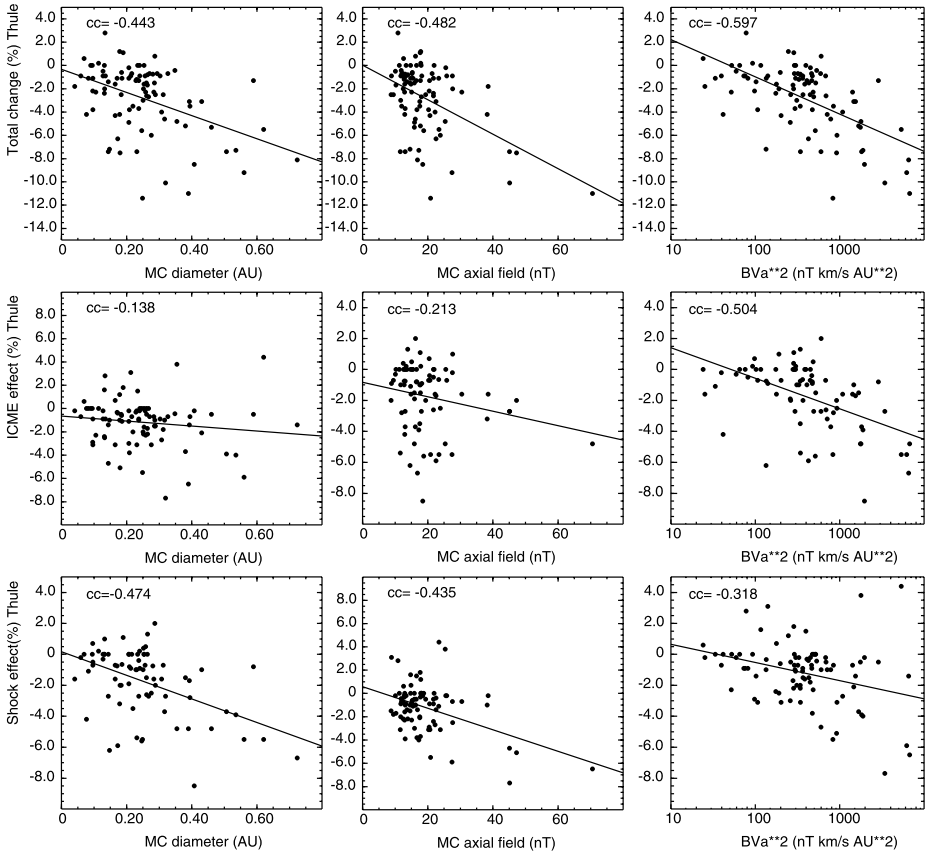

Figure 10 Total FD size and the sizes of the ICME and shock effects at Thule for magnetic clouds plotted against cloud diameter (a), axial magnetic field intensity (B) (estimates from the WIND magnetic cloud list), and BVa^2.

Another influence on FD size that is not reflected in the ICME parameters considered above is the possibility that GCRs flow into the ICME along open field lines that have reconnected with the IMF. We might expect ICMEs that contain a larger fraction of open *vs*. closed field lines to fill up more rapidly with GCRs, reducing the size of the intensity decrease observed as the ICME passes by. It is also possible that within the ICME, the decrease size may be larger in regions of closed field lines than in regions of open field lines such as reported by Bothmer *et al.* (1997).

One way of identifying open and closed field lines is to examine plots of the suprathermal electron intensity *versus* pitch angle and time, *e.g.*, (Shodhan *et al.*, 2000) who studied a sample of magnetic clouds observed by WIND. For the events in our study, we have used 2-minute averaged measurements of the suprathermal (272 eV) electron distribution function versus pitch angle made by the SWEPAM instrument on ACE and available from the ACE Science Center (http://www.srl.caltech.edu/ACE/ASC/DATA/level3/swepam/). In particular, we have compared the intensities of 272 eV electrons averaged over pitch angles of $0-27°$ (I_0), $81-99°$ (I_{90}) and $153-180°$ (I_{180}) with respect to the magnetic field direction (measurements are provided for twenty 9°-width ranges covering $0-180°$ in pitch angle).

Such intensities are shown for the ICME in Figure 2, where the black trace in the third panel from the bottom of the figure indicates I_0, the red trace is I_{90} and the green trace is I_{180}. We then required both $I_0/I_{90} \geq 2$ and $I_{180}/I_{90} \geq 2$ for a bi-directional flow. Comparison with plots of the SWEPAM pitch angle distributions (also available from the ACE Science Center) suggests that these criteria generally indicate regions of bi-directional flows that would be identified in these plots. In addition, estimates of the percentage of open and closed field lines for the events of Shodhan *et al.* (2000) that were also observed by ACE are similar to those they obtained and show consistent event-to-event trends. Note that these criteria do not require the parallel and anti-parallel electron flows to be approximately balanced (*i.e.*, $I_0 \sim I_{180}$) since observations (see, *e.g.*, Kahler, Crooker, and Gosling, 1999) indicate that this is frequently not the case. For example, the path length may be shorter to one footpoint of a looped field line than to the other footpoint, possibly resulting in a stronger anti-solar heat flux being observed from the direction of the closest footpoint.

The left-hand, center and right-hand panels of Figure 11 show the sizes of the total decrease, the shock effect and the ICME effect, respectively, measured by the IMP 8 guard or Thule NM plotted *versus* the percentage of the time when bi-directional 272 eV electrons were present during passage of the ICME, suggestive of the presence of looped rather than open field lines. We would of course expect the presence of open or closed field lines to influence most directly the size of the ICME effect. Specifically we might expect ICMEs with a greater presence of closed field lines (*i.e.*, bi-directional electrons) to tend to show larger GCR decreases. However, there is only a slight trend in this direction that is more evident in the guard data where the largest ICME effects are predominantly associated with ICMEs in which bi-directional electrons are observed for $> \sim 90\%$ of the time. Interestingly, such trends are stronger in the shock effect (which should not be influenced by the field configuration in the following ICME) and also in the total decrease. In addition, in all cases, relatively weak decreases occur irrespective of the prevalence of bi-directional electrons, so a predominance of bi-directional electrons (closed field lines) is not necessarily associated with a large GCR decrease.

Figure 12 illustrates that the percentage of time when bi-directional suprathermal electrons are present in an ICME shows a positive trend with *in situ* speed (the maximum speed in the sheath or ICME is shown here). In particular, the fastest events are predominantly associated with ICMEs that are filled with bi-directional electrons, and exceptionally fast events do not include ICMEs with predominantly open field lines. Such results are consistent with the expectation that there will be less time for reconnection to occur for the faster ICMEs. In contrast, slow ICMEs, below ~ 600 km s^{-1} range from predominantly open to predominantly closed. In summary, it is not clear whether the trend in FD size with the fraction of closed field lines suggested in Figure 11 is a reflection of the ability of particles to enter the ICME along reconnected field lines, or whether it arises because the FD size and fraction of bi-directional electrons in an ICME both increase for faster ICMEs.

We have also searched within our ICMEs for evidence of GCR intensity variations that are associated with transitions from regions of open to closed field lines, as indicated by unidirectional or bi-directional suprathermal electron flows, respectively. Similar features were observed by Bothmer *et al.* (1997) at *Ulysses* in the outer heliosphere and interpreted in terms of easier GCR entry into the ICME (and hence higher GCR intensity) on reconnected field lines compared to field lines rooted at the Sun at each end. However, we find that generally there is little evidence of changes in the GCR intensity in our ICMEs that are associated with changes in the electron flows in this way.

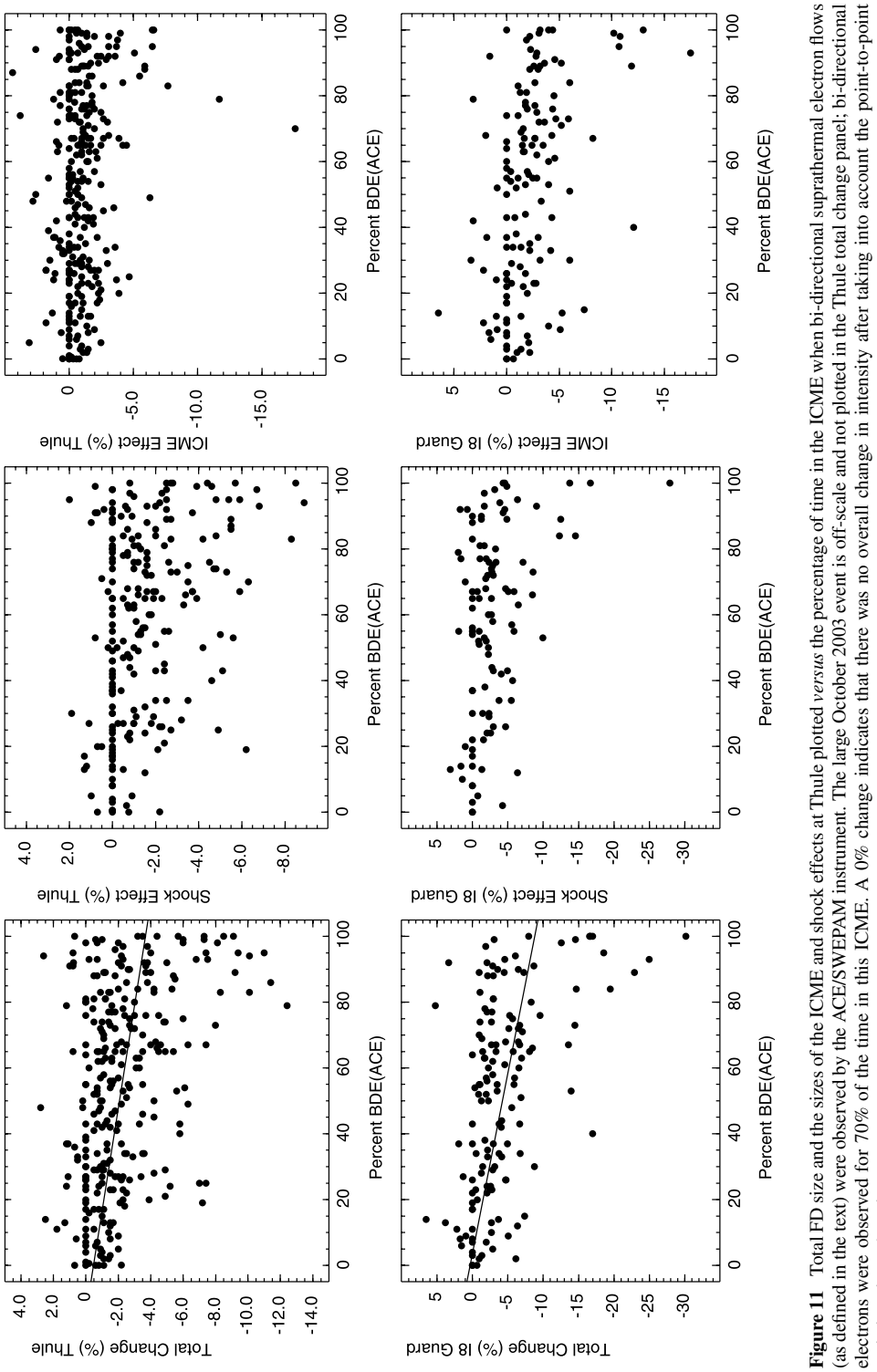

Figure 11 Total FD size and the sizes of the ICME and shock effects at Thule plotted *versus* the percentage of time in the ICME when bi-directional suprathermal electron flows (as defined in the text) were observed by the ACE/SWEPAM instrument. The large October 2003 event is off-scale and not plotted in the Thule total change panel; bi-directional electrons were observed for 70% of the time in this ICME. A 0% change indicates that there was no overall change in intensity after taking into account the point-to-point variations in each region.

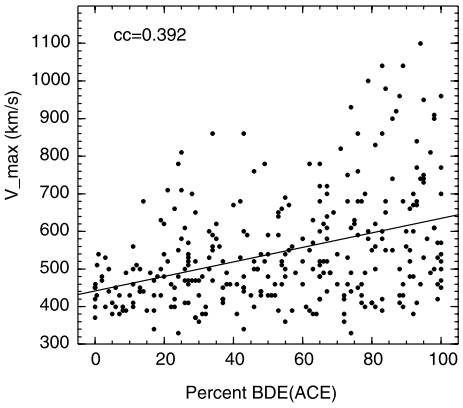

Figure 12 Maximum solar wind speed in the sheath or ICME plotted *versus* the percentage of time in the ICME when bi-directional suprathermal electron flows (as defined in the text) were observed by the ACE/SWEPAM instrument.

4. Summary and Discussion

Analysis of the response to the GCR intensity (as measured by the Thule neutron monitor (NM) or the IMP 8 GME guard) to the passage of ICMEs and the associated shocks in the vicinity of Earth during Solar Cycle 23 indicates that:

- Both the shock and ICME effects may contribute to the formation of Forbush decreases (FDs). On average, both contribute about equally. In around a quarter of events, the shock effect provides most of the FD, while in $\sim$20% of events, there is no shock effect, just the ICME effect.
- During the passage of 80 – 90% of ICMEs, minimum GCR intensity is found inside the ICME.
- The total FD size is better correlated with the ICME speed than other ICME parameters. The ICME effect has little dependence on the ICME axial field or diameter, or BVa^2, contrary to the expectation of simple FD models.
- There is a trend toward more magnetically closed ICMEs being associated with larger FDs. However, the fraction of closed field lines is also correlated with ICME speed, and the shock effect, so it is not clear that it is the ICME magnetic field topology as inferred from BDEs that directly influences the FD size.
- The largest FDs typically involve ICMEs that are magnetic clouds.

These results are consistent with our previous studies using single and multiple spacecraft observations that have clearly demonstrated the roles of both the shock and ICME effects in Forbush decreases (see, *e.g.*, Cane, 1993; Cane *et al.*, 1994; Cane, Richardson, and Wibberenz, 1997).

Recently, Reames, Kahler, and Tylka (2009) have questioned the role of ICMEs, specifically magnetic clouds, in producing particle intensity decreases including FDs. They examined observations of the intensities of anomalous cosmic ray (ACR) ^{4}He and O at a few MeV/n from the LEMT instrument on the WIND spacecraft and GCRs from the 121 – 230 MeV proton channel of the IMP 8 GME in the vicinity of 23 slow magnetic clouds with no or only weak preceding shocks identified by Shodhan *et al.* (2000). Such events are ideal for assessing the role of magnetic clouds in FDs since the shock effect should be absent or weak and the ICME effect should be dominant. Figure 13 shows four intervals including the passage of magnetic clouds discussed in Reames, Kahler, and Tylka (2009). The top panel of each pair shows ACR ^{4}He, O, and C at energies of a few MeV/n and (except for the top left) the 121 – 230 MeV proton intensity at IMP 8, as illustrated in Reames,

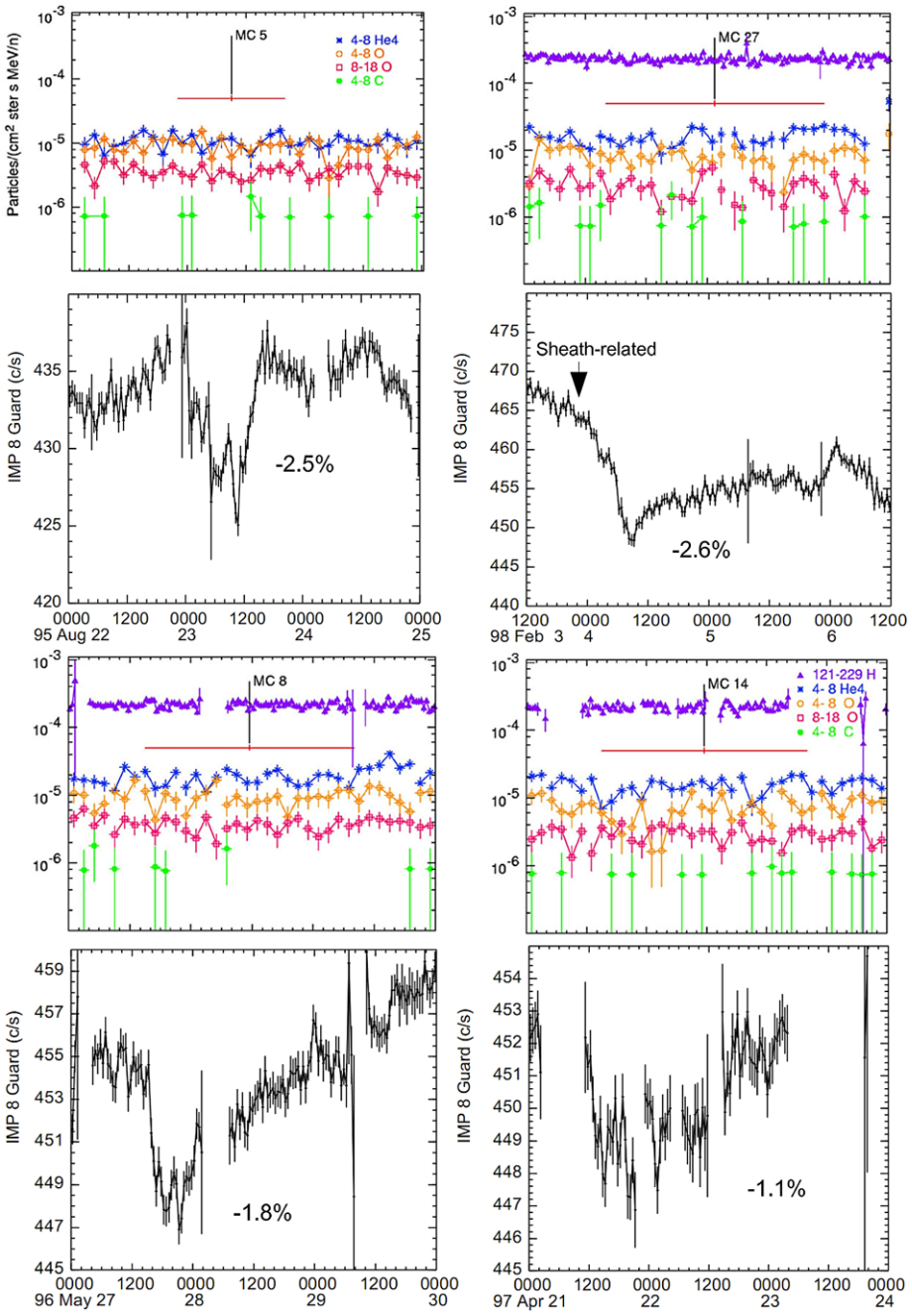

Figure 13 Four magnetic cloud events (Reames, Kahler, and Tylka, 2009) showing the 121 – 230 MeV proton intensity (except for the August 1995 event) and ACR ^{4}He, O and C as plotted in that paper. The lower panel of each pair shows the IMP 8 guard counting rate. In each case, the guard clearly shows a typical GCR intensity decrease of a few percent or so associated with passage of the magnetic cloud. These decreases are not evident in the 121 – 230 MeV proton data because of the larger statistical errors compared to the guard rate and compressed vertical scale.

Kahler, and Tylka (2009). The horizontal red line indicates passage of the magnetic cloud. Based on such data, Reames, Kahler, and Tylka (2009) concluded that "The MCs ... are uniformly populated with ACRs and GCRs. ... These observations argue against the existence of any dominant structures in the clouds that are magnetically closed to energetic ions above a few MeV amu^{-1}. [They] raise many significant new questions about the validity of contemporary views of particle transport and the topology of MCs."

We note, however, that the counting rate of the GME anti-coincidence guard shown in the bottom panel of each pair, not discussed by Reames, Kahler, and Tylka (2009), clearly shows a typical, few percent or so, local GCR decrease associated with the passage of each magnetic cloud. This is also the case for 23 of the other 26 magnetic clouds discussed by Reames, Kahler, and Tylka (2009). (The exceptions are: 2 June 1998 which shows an increase rather than a decrease in the guard rate; 7 August 1996, which shows a gradual decline in the guard rate over three days starting near the MC leading edge; and 9 June 1997 where there are significant guard data gaps.) Neutron monitor observations *e.g.*, from the Thule NM, also not considered by Reames, Kahler, and Tylka (2009), generally corroborate these conclusions. We have also previously discussed the cosmic ray depressions accompanying the Shodhan *et al.* (2000) magnetic clouds (Cane *et al.*, 2001). Thus we disagree with the conclusion of Reames, Kahler, and Tylka (2009) that these magnetic clouds were not associated with GCR decreases. We suggest that they were unable to detect the GCR decreases because the $\sim 10\%$ statistical error in the 30-minute averaged GME 121 – 230 MeV proton channel data that they used is too large to allow the few % depressions in the GCR intensity associated with passage of the magnetic clouds to be identified. Such variations also would be difficult to recognize with the compressed vertical scale used in their presentations in Figure 13. The depressions are, however, readily visible in the guard rate (statistical error $\sim 0.1\%$) when plotted with a suitable scale.

In conclusion, we do not agree with the claim of Reames, Kahler, and Tylka (2009) that our current view of the topology of magnetic clouds as inferred from energetic particle observations requires revision. Nevertheless, it is also clear from the observations in the present paper that the relationship between the properties of FDs and the *in situ* properties of ICMEs is still poorly understood, presumably because the properties of FDs are determined by large scale structures – the shock/sheath and ICME – but our *in situ* observations are typically made along just one trajectory through these structures. Additional modeling efforts, extending previous work such as discussed in the introduction, may help to provide the link between *in situ* observations and the global properties of ICMEs and their related shocks and sheaths that are fundamental to the formation of FDs.

Acknowledgements The Thule neutron monitor (PI: John Bieber) is supported by the University of Delaware and the Bartol Research Institute. Data were obtained from the Bartol website (http://neutronm.bartol.udel.edu/). We are indebted to the many experimenters who have contributed the near-Earth data used in the ICME identification.

References

Badruddin, Yadav, R.S., Yadav, N.R.: 1986, *Solar Phys.* **105**, 413.
Barnden, L.R.: 1973a, *Proc. 13th Int. Cosmic Ray Conf.* **2**, 1271.
Barnden, L.R.: 1973b, *Proc. 13th Int. Cosmic Ray Conf.* **2**, 1277.
Bothmer, V., Heber, B., Kunow, H., Müller-Mellin, R., Wibberenz, G., Gosling, J.T., Balogh, A., Raviart, A., Paizis, C.: 1997, *Proc. 25th Int. Cosmic Ray Conf.* **1**, 333.
Cane, H.V.: 1993, *J. Geophys. Res.* **98**, 3509.
Cane, H.V.: 2000, *Space Sci. Rev.* **93**, 55.

Cane, H.V., Richardson, I.G.: 2003, *J. Geophys. Res.* **108**, 1156.
Cane, H.V., Richardson, I.G., Wibberenz, G.: 1995, *Proc. 24th Int. Cosmic Ray Conf.* **4**, 377.
Cane, H.V., Richardson, I.G., Wibberenz, G.: 1997, *J. Geophys. Res.* **102**, 7075.
Cane, H.V., Richardson, I.G., von Rosenvinge, T.T., Wibberenz, G.: 1994, *J. Geophys. Res.* **99**, 21429.
Cane, H.V., Richardson, I.G., Wibberenz, G., Dvornikov, V.M., Sdobnov, V.E.: 2001, *Proc. 27th. Int. Cosmic Ray Conf.*, 3531.
Farrugia, C.J., Vasquez, B., Richardson, I.G., Torbert, R.B., Burlaga, L.F., Biernat, H.K., Mühlbachler, S., Ogilvie, K.W., Lepping, R.P., Scudder, J.D., Berdichevsky, D.B., Semenov, V.S., Kubyshkin, I.V., Phan, T.-D., Lin, R.P.: 2001, *Adv. Space Res.* **28**(5), 759.
Forbush, S.E.: 1937, *Phys. Rev.* **51**, 1108.
Gosling, J.T., Baker, D.N., Bame, S.J., Feldman, W.C., Zwickl, R.D.: 1987, *J. Geophys. Res.* **92**, 8519.
Hess, V.F., Demmelmair, A.: 1937, *Nature* **140**, 316.
Huttunen, K.E.J., Schwenn, R., Bothmer, V., Koskinen, H.E.J.: 2005, *Ann. Geophys.* **23**, 625.
Kahler, S.W., Crooker, N.U., Gosling, J.T.: 1999, *J. Geophys. Res.* **104**, 9911.
Klein, L.W., Burlaga, L.F.: 1982, *J. Geophys. Res.* **87**, 613.
Krittinatham, W., Ruffolo, D.: 2009, *Astrophys. J.* **704**, 831.
Kubo, Y., Shimazu, H.: 2010, *Astrophys. J.* **720**, 853.
Lockwood, J.A., Webber, W.R., Debrunner, H.: 1991, *J. Geophys. Res.* **96**, 11587.
McGuire, R.E., von Rosenvinge, T.T., McDonald, F.B.: 1986, *Astrophys. J.* **301**, 938.
Palmer, I.D.: 1982, *Rev. Geophys. Space Phys.* **20**, 335.
Reames, D.V., Kahler, S.W., Tylka, A.J.: 2009, *Astrophys. J. Lett.* **700**, L199.
Richardson, I.G.: 1997, In: Crooker, N., Joselyn, J.A., Feynman, J. (eds.) *Coronal Mass Ejections*, *AGU Geophys. Monogr.* **99**, 189.
Richardson, I.G.: 2004, *Space Sci. Rev.* **111**, 267.
Richardson, I.G., Cane, H.V.: 1995, *J. Geophys. Res.* **100**, 23397.
Richardson, I.G., Cane, H.V.: 2004, *J. Geophys. Res.* **109**, A09104.
Richardson, I.G., Cane, H.V.: 2010a, *Solar Phys.* **264**, 189.
Richardson, I.G., Cane, H.V.: 2010b, In: Maksimovic, M., Issautier, K., Meyer-Vernet, N., Moncuquet, M., Pantellini, F. (eds.) *Twelfth Int. Solar Wind Conf.*, *AIP Conf. Proc.* **1216**, 683.
Richardson, I.G., Cane, H.V., Wibberenz, G.: 1999, *J. Geophys. Res.* **104**, 12549.
Sanderson, T.R., Beeck, J., Marsden, R.G., Tranquille, C., Wenzel, K.-P., McKibben, R.B., Smith, E.J.: 1990, *Proc. 21st Int. Cosmic Ray Conf.* **6**, 251.
Shalchi, A., Büsching, I., Lazarian, A., Schlickeiser, R.: 2010, *Astrophys. J.* **725**, 2117.
Shodhan, S., Crooker, N.U., Kahler, S.W., Fitzenreiter, R.J., Larson, D.E., Lepping, R.P., Siscoe, G.L., Gosling, J.T.: 2000, *J. Geophys. Res.* **105**, 27261.
Simpson, J.A.: 1954, *Phys. Rev.* **94**, 426.
Vanhoefer, O.: 1996, Master's thesis, University of Kiel.
Wibberenz, G., le Roux, J.A., Potgieter, M.S., Bieber, J.W.: 1998, *Space Sci. Rev.* **83**, 309.
Zhang, G., Burlaga, L.F.: 1988, *J. Geophys. Res.* **93**, 2511.
Zurbuchen, T.H., Richardson, I.G.: 2006, *Space Sci. Rev.* **123**, 31.